Talanta 107 (2013) 297–303

Contents lists available at SciVerse ScienceDirect

Talanta

journal homepage: www.elsevier.com/locate/talanta

Single-molecule DNA digestion in various alkanethiol-functionalized gold nanopores

Seungah Lee, Seong Ho Kang*

Department of Applied Chemistry, College of Applied Science, Kyung Hee University, Yongin-si, Gyeonggi-do 446-701, Republic of Korea

ARTICLE INFO

Article history:
Received 9 November 2012
Received in revised form
14 January 2013
Accepted 15 January 2013
Available online 4 February 2013

Keywords:
Enzyme digestion
DNA
Nanopores
Alkanethiols
Single-molecule study

ABSTRACT

This paper presents the alkanethiol-functionalized environmental effects of individual DNA molecules in nanopores on enzyme digestion at the single-molecule level. A template consisting of gold deposited within a solid-state nanoporous polycarbonate membrane was used to trap individual λ-DNA and enzyme molecules. The gold surfaces were modified with various functional groups (–OH, –COOH, $–NH_3$). The enzyme digestion rates of single DNA molecules increased with decreasing nanopore diameters. Surprisingly, the digestion rates in the L-cysteine chemisorbed nanopores were 2.1–2.6 times faster than in the mercaptoethanol chemisorbed gold nanopores, even though these nanopores had equivalent interspacial areas. In addition, the membrane of chemisorbed cysteamine with ionized functional groups of H_3N^+ at pH 8.2 had a greater positive influence on the enzyme digestion rate than the membrane of chemisorbed mercaptoproponic acid with ionized carboxyl groups (COO^-). These results suggest that the three-dimensional environment effect is strongly correlated with the functional group in confined nanopores and can significantly change the enzyme digestion rates for nanopores with different internal areas.

1. Introduction

Most studies of single-molecule reactions have been conducted in free solutions. Single-molecule measurements have revealed information about the kinetic processes and the distribution of molecular properties within a large ensemble [1–5]. Of these single-molecule studies, single-molecule enzymatic assays have attracted the attention of many researchers [6–9]. In previous single-molecule DNA digestion studies, the enzyme hydrolysis of individual nucleotides was analyzed and identified using optical microscopy [10,11]. Depending on the single-molecule technique used, average DNA digestion rates of 12 bp/s [12], 15–20 bp/s [13], and 32 bp/s [14] have been reported in different confined environments with differing electrostatic, hydrophobic, and steric surface properties. However, the effects of a three-dimensional (3-D) environment on these rates at the single-molecule level are still not well understood.

The manipulation and control of molecules or ions through the use of nanoporous structures has been utilized in DNA translocation studies and in ultra-fast genome sequencing analysis [15–17]. In particular, the reaction mechanism of enzymatic DNA degradation in a confined environment is a key issue in the field of nanopore technology [18–20].

The goal of this work is to investigate the three-dimensional environmental effects of chemicals with various functional groups chemisorbed by nanopores on single-molecule DNA digestions. Specifically, alkanethiols ($HS–(CH_2)_n–R$), which have a thiol group on one end, spontaneously form bonds within gold (Au) nanopores. This spontaneous reaction organizes chains on the surface in a well-defined pattern with the variable head group (R) forming the surface of the monolayer. Therefore, alkanethiols with different terminal R-groups are important in determining the functionality and properties of the monolayer. The chemical environment within the Au nanopores can be altered by the chemisorption of mercaptoethanol (ME), cysteine, mercaptopropioinc acid (MPA), and cysteamine to the inner walls of the pores. The enzymatic digestions of DNA molecules trapped in the pores through interaction with the hydrophilic tail group (–OH, –COOH, $–NH_3$) were detected using the first optical imaging system to integrate total internal reflection fluorescence microscopy (TIRFM) and real-time confocal microscopy (RT-CM). This system was developed in our laboratory [21]. The activity of enzymatic digestion of DNA was analyzed at the single-molecule level by measuring the decreasing relative fluorescence intensity of fluorescent dye (YOYO-1)–DNA. In addition, the relationship between the digestion rate of DNA and the pore functional group was studied by varying the buffer solution pH using L-cysteine

* Corresponding author. Tel.: +82 31 201 3349; fax: +82 31 201 2340.
E-mail address: shkang@khu.ac.kr (S.H. Kang).

0039-9140/$ - see front matter © 2013 Elsevier B.V. All rights reserved.
http://dx.doi.org/10.1016/j.talanta.2013.01.046

chemisorbed polycarbonate (PC)/Au nanopores. The results demonstrated for the first time that individual DNA molecules had different enzyme digestion rates depending on the reaction conditions and the 3-D environment.

2. Materials and methods

2.1. Reagents and materials

Various track-etched PC membrane filters (Sterlitech Co., Kent, WA, USA), with various pore sizes (ϕ=200 nm–5.0 μm) and thicknesses (9–11 μm), were used as the synthetic pores. The λ-DNA (M_w=48,502 bp) was obtained from Promega (Madison, WI, USA). The λ-exonuclease enzyme (M_w=28 kDa, pI=5.5) was obtained from New England BioLabs (Ipswich, MA, USA). The H_2SO_4 and $SnCl_2$ were obtained from Fisher Scientific (Rockford, IL, USA). The trifluoroacetic acid, $AgNO_3$, Na_2SO_3, $NaHCO_3$, 37% formaldehyde, 99% mercaptoethanol (ME), 99% 3-mercaptopropinoic acid (MPA), and 98% cysteamine were obtained from Sigma-Aldrich. The commercial gold-plating solution ($Na_3Au(SO_3)_2$: Oromerse SO Part B) and 99% L-cysteine hydrochloride were obtained from Technic Inc. (Cranston, RI, USA) and TCI (Tokyo, Japan), respectively.

2.2. Preparation of samples

The λ-exonuclease (0.2 μg/mL) enzyme was diluted in a 1 × reaction buffer (pH 9.4, 2.5 mM of $MgCl_2$, 67 mM of glycine–KOH, 50 μg/mL of BSA). The λ-DNA was labeled with the YOYO-1 (Molecular Probes, Eugene, OR) intercalator at a molar ratio of 1:50 to minimize the photo-cleavage effect for the dye to nucleotide pairs (base pairs) in a 10 mM Gly–Gly buffer solution (pH 8.2) prior to enzyme digestion in a porous chamber. The DNA sample was further diluted to 1 pM using a suitable buffer solution (a 10 mM Gly–Gly solution buffered at pH 8.2 or a 20 mM sodium phosphate solution buffered at pH 2, 6, and 10) before the trapping process. All buffer solutions were filtered through a 0.2 μm membrane filter prior to use.

2.3. Electroless gold deposition and chemisorption

Gold was deposited in the pores and on the face of the PC template membrane using an electroless deposition method similar to that described previously [22]. The PC membrane was immersed in methanol for 5 min and then immersed in a solution of 0.026 M $SnCl_2$ and 0.07 M trifluoroacetic acid in 50% methanol for 45 min. The membrane was washed in methanol two consecutive times for 2.5 min and was then immersed in an aqueous ammoniacal $AgNO_3$ solution (0.035 M) for 5 min. After washing by immersion in water for 5 min, the membrane was placed in a Au-plating bath containing 7.7 mM $Na_3Au(SO_3)_2$, 0.127 M Na_2SO_3, 0.625 M formaldehyde, and 0.025 M $NaHCO_3$ (pH was adjusted to 10 by the dropwise addition of 0.5 M H_2SO_4) with constant stirring. The temperature of this bath was maintained at 2 °C for 12 h. The Au-deposited membranes were washed with water for 5 min and then dried at room temperature (Fig. 1A).

Chemical solutions were chemisorbed to the pore walls in order to change the chemical environment of the pore surface. L-cysteine chemisorption was accomplished by immersing the Au-deposited PC membranes in 2 mM L-cysteine hydrochloride in 80% ethanol for 24 h (Fig. 1A). The membrane was then rinsed with ethanol and dried in air. Thiol chemisorption was accomplished by immersing the Au-deposited PC membranes in a solution of 1 mM ME, 1 mM MPA, and cysteamine in absolute ethanol for 24 h (Fig. 1A). The membrane was then rinsed with ethanol and dried in air.

2.4. Characterization of Au nanoporous membrane filters

Field emission scanning electron microscope (FE-SEM) measurements were performed using a SUPRA 55 (Carl Zeiss) microscope in the secondary electron image mode in order to measure the membrane filter surface and pore diameter. The various functional groups of the Au deposited within the pores were confirmed by Fourier transform infrared (FT-IR) spectroscopy with an advanced grazing angle (PIKE Technologies Inc., Madison, WI, USA). All measurements were performed at room temperature.

2.5. Trapping and digestion of individual DNA molecules

Note that thiols with hydrophobic properties, propanethiol, decanethiol, and hexadecanethiol, chemisorbed to the inside of nanopores do not permit trapping of hydrophilic species (i.e., buffer solution, DNA, and enzyme molecules). However, the ME and L-cysteine chemisorbed PC/Au membranes were hydrophilic with wetting characteristics that helped the filters stick to the surface of the cover glass (22 × 60 mm) (Fig. S1, Electronic Supplementary Information). A suitable buffer solution (pH 2, 6, 8.2, and 10) was added to the center of the membrane filter on the cover glass such that it perfectly adhered to the surface. The cover glass was matched with immersion oil (n=1.78, Cargille Labs, NJ, USA) on the objective lens made for total internal reflection fluorescence (TIRF). Individual DNA molecules were easily trapped and digested by the following procedure. First, 2 μL of DNA diluted to 1 pM using the appropriate buffer solution was added to the nanopore chambers. Subsequently, a 0.2 μg/mL enzyme in a 1 × reaction buffer solution was added to the region between the chemisorbed PC/Au membrane and the cover glass (ϕ=12 mm) using capillary force. The λ-exonuclease enzyme digestion rate was measured from the integrated TIRF and confocal fluorescence intensity of a single coiled DNA in the nanopore chamber at 37 °C (Fig. 2B). The homogeneity and purity of the λ-exonuclease was confirmed by slab gel electrophoresis (Fig. S2, Electronic Supplementary Information).

2.6. Optical imaging system integrated by TIRFM and RT-CM

A modified integrated optical imaging system [21] was used for real-time detection of single molecules. Construction of the hybrid TIRFM and RT-CM with a conventional epifluorescence microscope is shown in Fig. 2A. An Olympus IX71 inverted microscope (Olympus Optical, Tokyo, Japan), coupled with a Plan Apo 100 × /1.65 HR objective lens (W.D.=0.10 mm, oil type, Olympus), used transmitted light to visualize the morphology of the nanoporous chamber. A 473 nm laser (SL-473 nm-50T, Shanghai Laser Century Technology Co., Ltd., China) was used as the light source for TIRFM studies. The filter cube was composed of 520/15 nm bandpass filters (Olympus). The optical system was integrated with the confocal system by mounting confocal scanners (CSU 22, Yokogawa Electric Co., Tokyo, Japan) on the inverted microscope platform of an Olympus IX71. A 488 nm argon ion laser (35-LAB-431-220, Melles Griot) was used as the excitation source for the real-time confocal studies. A cooled charge-coupled device (CCD) camera (Cascade 512B, Photometrics, Tucson, AZ, USA) was mounted on the microscope confocal scanner. The CCD exposure time was 100 ms. The temperature of the membrane pores was maintained at 37 °C using a temperature controller (CU-105, Live Cell Instruments, Seoul, Korea) that was placed on the microscope stage for the enzyme reactions. To reduce photobleaching, a UNIBLITZ mechanical shutter (model LS3Z2, Vincent Associates, Rochester, NY, USA) with a VCM-D1 shutter driver (Vincent Associates) was used to block the laser beam when the

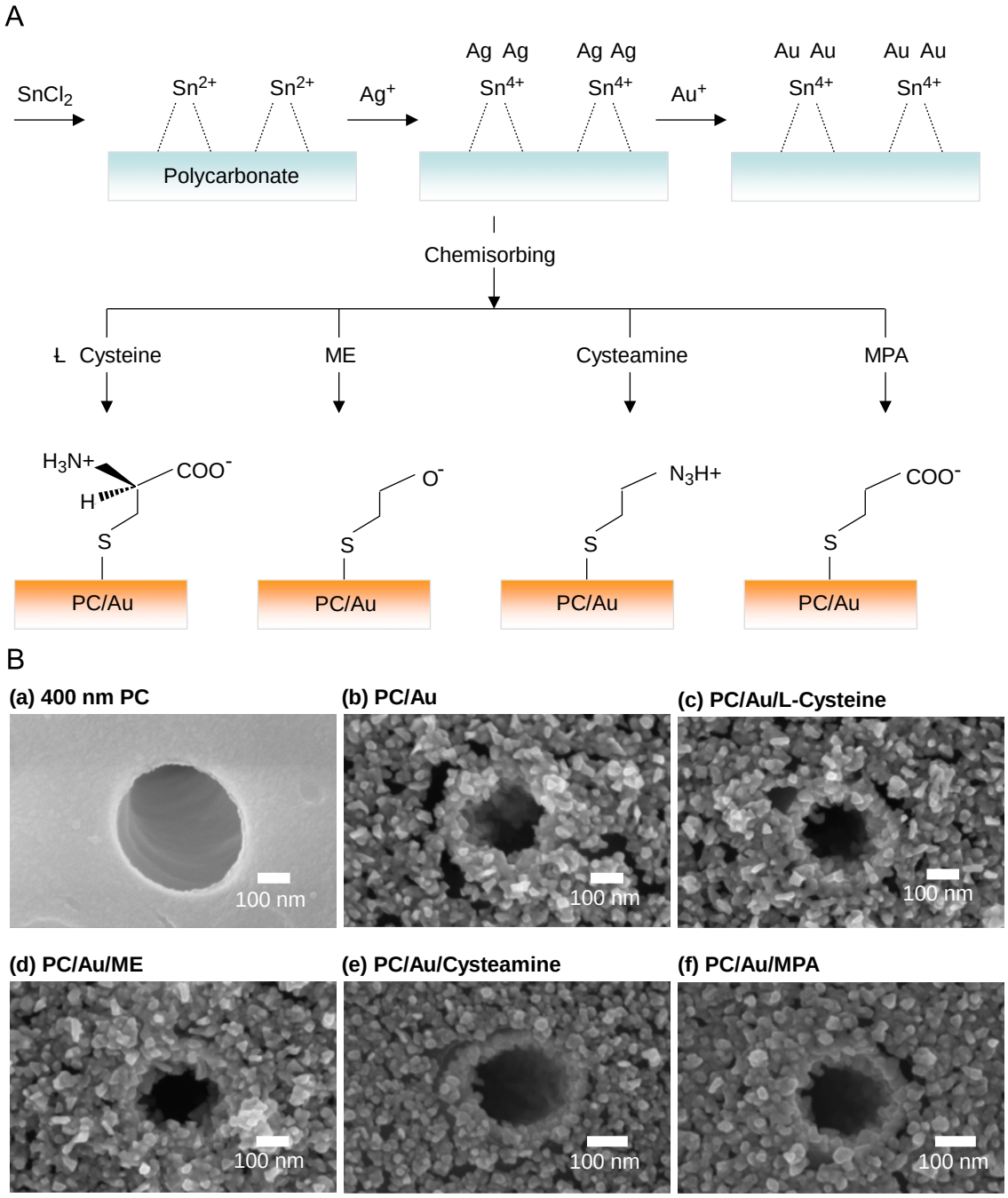

Fig. 1. (A) Schematic diagram of the electroless procedure used to deposit Au in the nanopores and (B) morphologies of the 400 mm-diameter PC (a), Au-deposited 400 nm PC (b), L-cysteine chemisorbed 400 nm PC/Au (c), mercaptoethanol chemisorbed 400 nm PC/Au (d), cysteamine chemisorbed 400 nm PC/Au (e), and mercaptopropioinc acid chemisorbed 400 nm PC/Au (f) by FE-SEM.

camera was off. Total internal reflection (TIR) and confocal fluorescence signals were corrected by subtracting the background noise. To correct the decreasing fluorescence signal in the TIRFM and confocal system images, we performed the following steps. First, we selected signal regions and background regions with the same area. Then, we calculated a sum of the fluorescence intensities of the occupied pixels for one DNA which had been corrected using background subtraction. We employed the MetaMorph 7.1 software (Universal Imaging Co., Downingtown, PA, USA) for all the quantitative analysis of the data and the image acquisition. Finally, we fit the enzymatic digestion rates of individual λ-DNA molecules by λ-exonuclease using Microsoft Excel software. A straight line was fitted to the decreasing fluorescence signal detected by TIRFM and RT-CM, and the slope was used to estimate the digestion rate.

3. Results and discussion

3.1. Characterization of porous membrane chambers

Fig. 1B shows the surface morphologies of the track-etched PC membrane, the PC/Au membrane, and the chemisorbed membrane as imaged by FE-SEM. The thickness of the Au layer deposited on the pore walls was controlled by varying the plating time [22]. The PC membrane pore diameter decreased to about

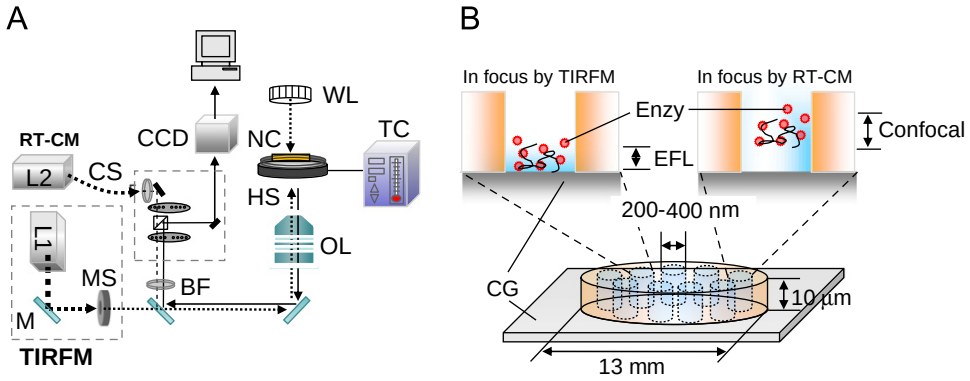

Fig. 2. (A) Schematic diagram of the integrated TIRFM and RT-CM optical imaging system. (B) Focal plane of a single DNA digestion by λ-exonuclease enzyme as observed by the TIRFM and RT-CM system. L1: TIRF laser source; L2: confocal laser source; M: mirror; MS: mechanical shutter; BF: bandpass filter; TC: temperature controller; OL: objective lens; NC: nanoporous chamber; WL: white light; CCD: charge-coupled device; CS: confocal scanner; HS: heating stage; EFL: evanescent field layer; Enzy: enzyme; CG: cover glass.

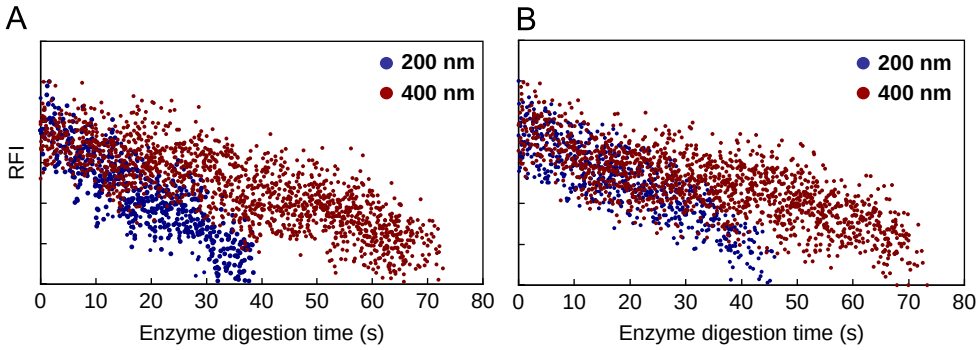

Fig. 3. Individual λ-DNA digestion rates in different nanopore sizes with respect to decreasing fluorescence intensity, as determined by (A) TIRFM and (B) RT-CM. The blue circles indicate 200 nm pores while the red circles denote 400 nm pores. (For interpretation of the references to color in this figure legend, the reader is referred to the web version of this article.)

200 nm from 400 nm due to Au deposition (Fig. 1B(b)). Alkanethiols with different terminal R-groups were chemisorbed onto the Au surface of the PC/Au membrane in order to investigate the enzyme digestion rate under different 3-D environments. The diameter of the pores of the Au-deposited membrane slightly decreased (by ~0.2 nm) after L-cysteine chemisorption (Fig. 1B(c)) [23]. In a report by Hou et al., Au deposition (at 1 °C for 0.5 h) reduced the pore radius by 2 nm, and formation of self-assembled monolayers (SAMs) with $HS(CH_2)_{11}$–OH onto the gold surface further reduced the pore radius by 1.5 nm [24]. Chemisorption with the shorter ME ($HS(CH_2)_2$–OH) reduced the pore radius by less than 1.5 nm (Fig. 1B(d)). FT-IR spectra showed the characteristic band of the functional group chemisorbed on the Au surface of the PC/Au membrane (Fig. S3).

3.2. Trapping of single molecules in membrane chambers

PC/Au membrane filters with different modified chemical groups were selected in order to observe the digestion rates of individual DNA molecules trapped in different environments. Since the surface of the chamber wall and its environment affect the detection of DNA molecules, the chamber diameter must be large enough to allow effective molecule entrapment but small enough that the chamber allows only one molecule to enter. Fig. S4 shows TIRF and confocal fluorescence images (Fig. S4A and C) of a single DNA molecule trapped within the pore, as well as bright field optical images of the PC/Au/cysteine membrane (Fig. S4B and D). These images confirm that an individual DNA molecule was effectively trapped in the chambers until a pore diameter of 200 nm was reached.

3.3. Enzyme digestion rates of single DNA molecules by two detection methods

Digestion of individual λ-DNA molecules with λ-exonuclease was indicated by decreasing the TIRF and confocal fluorescence intensities in each nano-sized chamber. For all the conditions studied, the fluorescence intensities decreased with the increasing enzyme digestion times of the individual DNA molecules trapped within the pore, except for the results under control conditions (no enzyme and no magnesium). There was no change in the fluorescence intensity under the control conditions, i.e., the average slope value of the least-squares regression line for the control signal was -0.09 ± 0.07 ($n=5$). The fluorescence intensities of the individual DNA molecules on a glass surface produced a similar digestion pattern to that of the molecules inside the nanopores (Figs. 3 and 4).

The enzyme digestion rate of single DNA molecules was calculated by two methods (TIRFM and RT-CM), and the significance of any difference (d_i) between the methods was determined using a paired Student's t test. The value of $t_{calculated}$ was found to be 0.15 for chemisorbed ME and 3.6 for chemisorbed L-cysteine, according to the following formula:

$$t_{calculated} = (|\bar{d}|/S_d)(n)^{1/2}$$

where $|\bar{d}|$ is the absolute value of the mean difference.

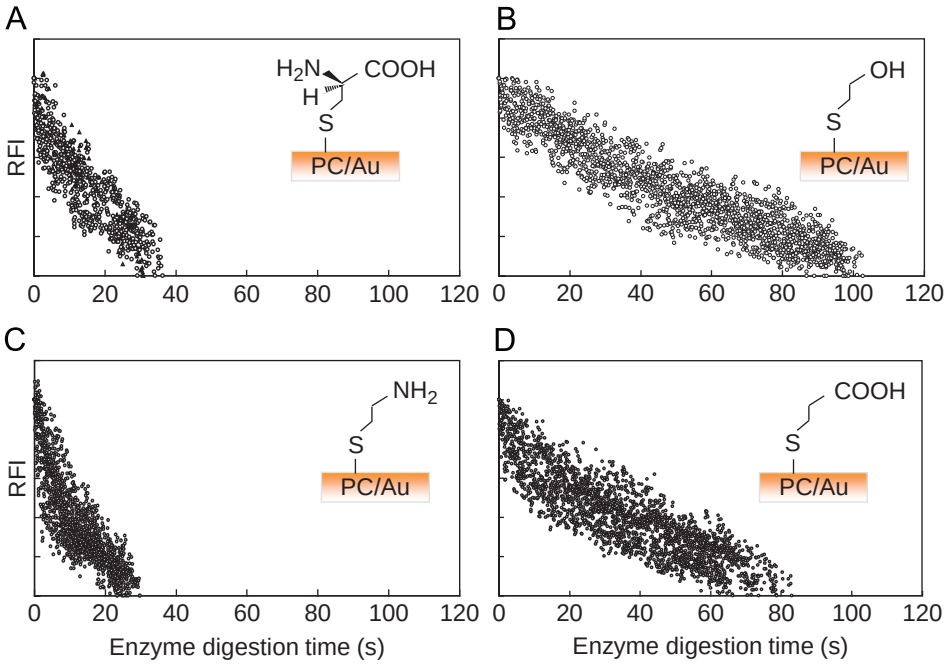

Fig. 4. Real-time digestion of individual λ-DNA molecules by a λ-exonuclease enzyme with respect to decreasing TIR fluorescence intensities according to various functional groups in PC/Au membrane nanopores modified by (A) L-cysteine, (B) ME, (C) cysteamine, and (D) MPA. The relative fluorescence intensity (RFI) values were calculated from the fluorescence intensities after subtracting the background noise.

The $t_{calculated}$ was less than t_{table} (3.747) at the 98% confidence level. In other words, the difference between the digestion rates found by the two detection methods was not significantly different at the 98% confidence level.

3.4. Enzyme digestion rates of single DNA molecules in a restricted area

The enzyme digestion rate of a single DNA molecule was predicted to increase with a decrease in the internal area of the nanopores in the same environment as a result of diffusional mixing of the solution components (Mg^{2+} ion, enzyme, etc.) during enzyme digestion (see Fig. 3 and Table 1). The enzyme digestion rates in the 200 nm nanopores were about 1.64–1.98 times faster than in the 400 nm nanopores. These data suggested that ion transport in the pore decreased according to the hindered diffusion of an unbounded solution that has been described in previous reports [25,26]. More specifically, Mg^{2+}, the cofactor in the 1 × exonuclease reaction buffer, may have more effectively activated the enzyme reaction due to the shorter diffusional distances in the smaller pore size, which would have led to a faster digestion rate of the individual DNA molecules by λ-exonuclease (Fig. 5).

3.5. Enzyme digestion of dependence for different functional groups

Surprisingly, the chemically-modified PC/Au surfaces showed different enzyme digestion rates in nanopores of the same size but with different functional groups. For example, the enzyme digestion rate of λ-DNA in L-cysteine chemisorbed nanopores was faster than in ME chemisorbed nanopores (Table 1; Figs. 4A, B and S5). In general, the ionized carboxyl and hydroxyl groups did not interact electrostatically with the DNA molecules since the DNA was negatively charged. However, the Mg^{2+} in the 1 × exonuclease reaction buffer was more easily attracted to L-cysteine chemisorbed nanopores due, most likely, to the greater acidity of the carboxyl group compared to the hydroxyl group (e.g., inductive effect and resonance effect), which thereby promoted the enzymatic reaction.

Table 1
Enzymatic digestion rates[a] of individual λ-DNA molecules by λ-exonuclease in chemisorbed-PC/Au membranes and in various nanopores based on the decrease in relative fluorescence intensity (RFI). λ-DNA molecules were labeled with YOYO-1 (dye:bp = 1:50, mol/mol).

Chemisorbed	Pore size (ϕ)	Detection method	
		TIRFM	Confocal
L-Cysteine	~200 nm[b]	1292 ± 198 bp/s (0.44 ± 0.07 μm/s)	1059 ± 50.8 bp/s (0.36 ± 0.02 μm/s)
Mercaptoethanol	~200 nm[b]	491.7 ± 18.5 bp/s (0.17 ± 0.01 μm/s)	496.3 ± 65.0 bp/s (0.17 ± 0.02 μm/s)
Carboxylate[c]	200 nm	1389 ± 205 bp/s (0.47 ± 0.07 μm/s)	1117 ± 101 bp/s (0.38 ± 0.03 μm/s)
Carboxylate[d]	400 nm	701.5 ± 37.0 bp/s (0.24 ± 0.01 μm/s)	681.3 ± 24.5 bp/s (0.23 ± 0.01 μm/s)

The enzymatic digestion rates were calculated using the length of a single λ-DNA molecule (48,502 bp = 16.5 μm) and the enzyme reaction time until the TIRF signal of DNA–YOYO-1 disappeared. The other conditions were the same as described in Figs. 3 and 4.

[a] Mean ± standard deviation (n = 5).
[b] 400 nm PC membrane is reduced to about 200 nm in diameter by deposition and chemisorption with Au and chemicals (Fig. 1B).
[c] 200 nm Polycarbonate (PC) membrane without chemisorption by chemicals and not deposited by Au.
[d] 400 nm PC membrane without chemisorption by chemicals and not deposited by Au.

L-Cysteine is a small, zwitterionic molecule with many potential intermolecular interactions governing its adlayer structure. The molecular features and adlayer structure of L-cysteine have been previously exploited on solid surfaces. For example, a SAM of L-cysteine on a Au surface was used to immobilize protein molecules [27,28] and to evaluate electrochemical quartz crystal microbalance data [29]. In addition, zwitterionic L-cysteine was used as a model for pH-switchable ion transport and selectivity in

Pore size (μm)	PC pore (bp/s)	Free solution[a] (bp/s)
5.0	209.3±16.0	175.4±27.9
1.0	223.2±28.5	
0.8	629.7±74.0	
0.6	1,325±78.2	

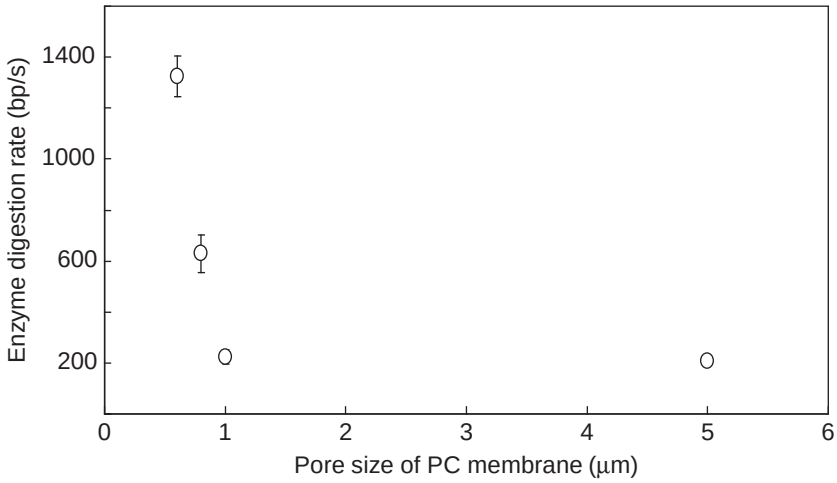

Fig. 5. Enzymatic digestion rates of individual λ-DNA molecules labeled with YOYO-1 (50:1) by λ-exonuclease in various PC pore sizes with respect to decreasing TIRF intensities. (a) The free solution corresponds to the observation of DNA molecules on the poly-L-lysine-coated glass. Enzyme digestion rates were calculated using the length of a single λ-DNA molecule (48,502 bp=16.5 μm) and the enzyme reaction time until the TIRF intensity of the DNA–YOYO-1 disappeared. The substrate used a cover glass immersed into a 0.1% poly-L-lysine solution.

a nanopore [30]. This membrane-chemisorbed L-cysteine had two ionized functional groups (COO^- and H_3N^+), since pH 6.0 is near the isoelectric point of chemisorbed L-cysteine [23]. The membrane wetted in a pH 8.2 buffer solution had a greater number of ionized carboxylate groups than charged ammonium groups. However, a few positively charged ammonium groups preferentially congregated the DNA and enzymes into the pore inner walls.

Alkanethiol SAMs are commonly used as model surfaces for surface plasmon resonance spectroscopy since they form stable, well-ordered monolayers on Au [31–33]. The surface modification of COOH- and NH_2-terminated SAMs have been used for the attachment of biopolymers such as oligonucleotides and peptides onto Au surfaces [34,35]. PC/Au chemisorbed with different terminal R-group alkanethiols was used to investigate the influence of functional groups on the enzymatic digestion of DNA molecules in a restricted area. Fig. 4C and D shows the enzymatic digestion rates of single DNA molecules chemisorbed by two different functional groups in different environments. The pK value of the MPA SAMs was reported to be 6.0 [36], indicating that the SAMs would be negatively charged under basic conditions (pH 8.2) by the deprotonation of the carboxylic acid groups to carboxylates. The use of cysteamine, which has a pK=8.6 [37] and a positively charged environment due to protonation at a pH of 8.2, resulted in a lack of repulsive electrostatic interactions between the molecules and the pore. The enzymatic digestion rate of the membrane chemisorbed with cysteamine (1846.7 ± 79.2 bp/s) was three times faster than that of the membrane chemisorbed with MPA (619.1 ± 71.6 bp/s).

These variations in the enzymatic digestion rates can be ascribed to electrostatic interactions between DNA molecules and the interiors of the membrane pores. The final pH values resulting from the mixture of the enzyme digestion buffer and various pH buffer solutions are shown in Fig. S6A. The enzyme displayed optimal activity for the pH values from 9.2 to 9.5. At the pH values of 7.0, 8.0, 10, and 10.2 the rates were 16%, 35%, 35%, and 8%, respectively [38]. Although the nanopores could have had large positive charges due to the presence of protonated amino groups at a pH of 2.0, the low pH inhibited the active center of the enzyme. Thus, enzyme digestion rates at low pH values could not be obtained. Furthermore, L-cysteine chemisorbed nanopores had more negative charges at high pH values, which are unfavorable to trapping DNA molecules. As a result, the enzyme digestion rate was higher at a pH of 8.2 than at pH values of 6.0 and 10 (Fig. S6B).

4. Conclusions

The 3-D environments of nanopores, which were examined by varying the functional group, hydrophilicity, pH, and internal area, was found to play an important role in enzyme digestion rates due to the interactions between the nanopore surface and the DNA molecule. The digestion rates of individual λ-DNA molecules were measured using an integrated TIRFM and RT-CM optical imaging system. The digestion rates for the two detection methods were not significantly different at the 98% confidence level. The enzymatic digestion of λ-DNA in L-cysteine chemisorbed nanopores was 2.1–2.6 times faster than in ME chemisorbed nanopores. In addition, the membrane chemisorbed with cysteamine (H_3N^+) at a pH of 8.2 had a more positive influence on the enzymatic digestion rate relative to the membrane chemisorbed with MPA (COO^-). The effect of functional groups on the enzymatic digestion rate of trapped DNA

molecules was observed more clearly in extremely restricted 3-D environments with chemically modified nanopore surfaces. Consequently, the electrostatic interaction between a molecule and a nanopore may be one of the most important factors determining enzymatic digestion rates. These results are comparable to those of previous studies of single-molecule DNA enzymatic digestion rates, which were reported to be 13–32 bp/s and ~100 bp/s under different conditions [10,16,39]. In addition, the digestion rate in 200-nm diameter nanopores was two times faster than in 400-nm diameter nanopores, presumably due to the shorter diffusional distances. Thus, the controlled 3-D environment of the nanopore significantly influences the enzymatic digestion rate of single DNA molecules.

Acknowledgments

This research was supported by a post-doctoral fellowship grant from Kyung Hee University in 2012 (KHU-20120350).

Appendix A. Supporting information

Supplementary data associated with this article can be found in the online version at http://dx.doi.org/10.1016/j.talanta.2013.01.046.

References

[1] J.J. Macklin, J.K. Trautman, T.D. Harris, L.E. Brus, Science 272 (1996) 255.
[2] T. Ha, T. Enderle, D.S. Chemla, P.R. Selvin, S. Weiss, Phys. Rev. Lett. 77 (1996) 3979.
[3] Q.F. Xue, E.S. Yeung, Nature 373 (1995) 681.
[4] D.B. Craig, E.A. Arriaga, J.C.Y. Wong, H. Lu, N.J. Dovichi, J. Am. Chem. Soc. 118 (1996) 5245.
[5] H.P. Lu, X.S. Xie, J. Phys. Chem. B 101 (1997) 2753.
[6] W. Tan, E.S. Yeung, Anal. Chem. 69 (1997) 4242.
[7] R.D. Vale, T. Funatsu, D.W. Pierce, L. Romberg, Y. Harada, T. Yanagida, Nature 380 (1996) 451.
[8] H.P. Lu, L. Xun, X.S. Xie, Science 282 (1998) 1877.
[9] S.H. Kang, S. Lee, E.S. Yeung, Analyst 135 (2010) 1759.
[10] S. Matsuura, J. Komatsu, K. Hirano, H. Yasuda, K. Takashima, S. Katsura, A. Mizuno, Nucleic Acids Res. 29 (2001) e79.
[11] Y. Tachiiri, M. Ishikawa, K. Hirano, Anal. Chem. 72 (2000) 1649.
[12] T.T. Perkins, R.V. Dalal, P.G. Mitsis, S.M. Block, Science 301 (2003) 1914.
[13] K. Subramanian, W. Rutvisuttinunt, W. Scott, R.S. Myers, Nucleic Acids Res. 31 (2003) 1585.
[14] A.M. Van Oijen, P.C. Blainey, D.J. Crampton, C.C. Richardson, T. Ellenberger, X.S. Xie, Science 301 (2003) 1235.
[15] A.S. Panwar, M. Muthukumar, J. Am. Chem. Soc. 131 (2009) 18563.
[16] G.V. Soni, A. Meller, Clin. Chem. 53 (2007) 1996.
[17] S.H. Kang, S. Lee, E.S. Yeung, Angew. Chem. Int. Ed. 49 (2010) 2603.
[18] S. Benner, R.J. Chen, N.A. Wilson, R. Abu-Shumays, N. Hurt, K.R. Lieberman, D.W. Deamer, W.B. Dunbar, M. Akeson, Nat. Nanotechnol. 2 (2007) 718.
[19] S.L. Cockroft, J. Chu, M. Amorin, M.R. Ghadiri, J. Am. Chem. Soc. 130 (2008) 818.
[20] N. Hurt, H. Wang, M. Akeson, K.R. Lieberman, J. Am. Chem. Soc. 131 (2009) 3772.
[21] S. Lee, S.H. Kang, Biosens. Bioelectron. 31 (2012) 393.
[22] K.B. Jirage, J.C. Hulteen, C.R. Martin, Anal. Chem. 71 (1999) 4913.
[23] S.B. Lee, C.R. Martin, Anal. Chem. 73 (2001) 768.
[24] Z. Hou, N.L. Abbot, P. Stroeve, Langmuir 16 (2000) 2401.
[25] W.M. Deen, AIChE J. 33 (1987) 1409.
[26] R.E. Beck, J.S. Schultz, Science 170 (1970) 1302.
[27] P. Tengvall, B. Liedberg, I. Lundstrom, Langmuir 8 (1992) 1236.
[28] Q.M. Xu, L.J. Wan, C. Wang, C.L. Bai, Z.Y. Wang, T. Nozawa, Langmuir 17 (2001) 6203.
[29] A.J. Tudos, P.J. Vandeberg, D.C. Johnson, Anal. Chem. 67 (1995) 552.
[30] P. Ramirez, S. Mafé, A. Alcaraz, J. Cervera, J. Phys. Chem. B 107 (2003) 13178.
[31] M. Besenicar, P. Macek, J.H. Lakey, G. Anderluh, Chem. Phys. Lipids 141 (2006) 169.
[32] E. Ostuni, L. Yan, G.M. Whitesides, Colloids Surf. B: Biointerfaces 15 (1999) 3.
[33] A. Subramanian, J. Irudayaraj, T. Ryan, Biosens. Bioelectron. 21 (2006) 998.
[34] M.C. Pirrung, Angew. Chem. Int. Ed. 41 (2002) 1276.
[35] E.A. Smith, M.J. Wanat, Y. Cheng, S.V.P. Barreira, A.G. Frutos, R.M. Corn, Langmuir 17 (2001) 2502.
[36] K. Kim, J. Kwak, J. Electroanal. Chem. 512 (2001) 83.
[37] M. Manuszak, E. Borish, R.R. Wickett, J. Soc. Cosmet. Chem. 47 (1996) 213.
[38] 〈http://www.neb.com〉.
[39] H. Kurita, K. Inaishi, K. Torii, M. Urisu, M. Nakano, S. Katsura, A. Mizuno, J. Biomol. Struct. Dyn. 25 (2008) 473.